Carbohydrate Polymers 115 (2015) 715–722

Contents lists available at ScienceDirect

Carbohydrate Polymers

journal homepage: www.elsevier.com/locate/carbpol

Synthesis of a microhydrogel composite from cellulose nanowhiskers and starch for drug delivery

Marcos R. Mauricio, Pablo G. da Costa, Shirani K. Haraguchi, Marcos R. Guilherme, Edvani C. Muniz, Adley F. Rubira*

Grupo de Materiais Poliméricos e Compósitos (GMPC) – Department of Chemistry, State University of Maringá, Av. Colombo, 5790, CEP 87020-900 Maringá, Paraná, Brazil

ARTICLE INFO

Article history:
Received 6 May 2014
Received in revised form 12 July 2014
Accepted 30 July 2014
Available online 7 August 2014

Keywords:
Cellulose
Drug delivery
Microparticles
Nanowhiskers
Starch

ABSTRACT

This work describes the preparation of a microhydrogel composite from cellulose nanowhiskers (CNW) and starch in an ultrasound assisted-emulsion. CNW, which showed rod-like morphology, was obtained by acid hydrolysis of cane-based cellulose. The introduction of vinyl bonds to both CNW and starch enabled us to create the microhydrogel composite in which CNW played a role as a covalent cross-linker. Furthermore, CNW may act as an emulsifying agent for emulsion, improving both sphericity and homogeneity of the microparticles. The drug release was regulated in response to changes in the CNW amounts. The modeling of the release kinetics indicated that the drug release is driven by an anomalous mechanism and that the addition of CNW to starch microparticles led to differences in that mechanism. The release rate became ca. 2.9 times slower when CNW is added. When combined with starch, CNW played a role as a retardant factor for drug release.

1. Introduction

For several years, many drugs have been developed to be absorbed in the gastrointestinal tract (GI), which comprises both the stomach and the intestine. GI is, in most cases, the site more appropriate for orally administrated drugs. The action of certain drugs can be improved when they are absorbed in the large intestine (colon). However, upon contact with the stomach and thin intestine environments, some drugs can undergo hydrolysis, affecting their therapeutic properties before reaching the colon (Shalviri et al., 2013; Zhang et al., 2013). Some approaches based on pH-responsive synthetic polymers and on polysaccharides, such as starch, have been proposed to overcome that limitation. For use in oral drug delivery systems, starch takes vantage of being resistant to gastric juice (Saboktakin, Tabatabaie, Maharramov, & Ramazanov, 2011).

The polysaccharides show great importance in the biomedical sector owing to a wide variety of potential applications including in the targeted delivery of drugs (Mauricio, Guilherme, Kunita, Muniz, & Rubira, 2012; Wu et al., 2011). Starch and cellulose, the latter being a material with nanocrystalline structures, are the most abundant polysaccharides in nature. Beyond being obtained from renewable sources, both materials offer other important advantages such as low cost, ease of chemical modification, ability to replace some synthetic polymers, good mechanical resistance and plasticity, and so on (Klemm et al., 2011; Olivato, Müller, Carvalho, Yamashita, & Grossmann, 2014; Sun, Fan, & Xiong, 2014; Wang et al., 2012).

The use of cellulose nanowhiskers (CNW) for developing biocomposites has been the target of current investigations (Chen et al., 2014; Dufresne, 2010; Habibi & Dufresne, 2008; Li, Ko, & Hamad, 2013). Sugarcane bagasse is a resource rich in cellulose. It is composed of lignin (ca. 15%), hemicelluloses (ca. 30%), and cellulose (ca. 40%). Cellulose is extracted from sugarcane bagasse by disrupting the complex of lignocellulose-polyose via delignification. Nanowhiskers with different levels of crystallinity may be obtained via cellulose hydrolysis. The sugarcane bagasse-derived CNW are viable from an economical point of view, owing to an increase in the production of sugarcane in the last years for cane-based alcohol. This led to an expressive increase in the discarded residues, the most part being bagasse.

The disadvantage of a biocomposite composed of starch is that it has a low water-solubility, limiting its processing in aqueous environments. To increase solubility of starch in water, some approaches based on chemical modification of the polysaccharide backbone have been proposed. The chemically modified starch

* Corresponding author. Tel.: +55 44 3011 3686.
E-mail address: afrubira@uem.br (A.F. Rubira).

http://dx.doi.org/10.1016/j.carbpol.2014.07.063
0144-8617/

could be used in the production of biocompatible, hydrophilic materials like covalent hydrogels (Ismail, Irani, & Ahmad, 2013; Pereira et al., 2013; Valiki & Rahneshin, 2013).

The hydrogels have markedly different properties when their size toward microscale. For example, the higher surface area of these materials at a microscale level (called microhydrogels) makes easier their interaction with the physiological environment, which is rich in water. Efficient strategies have been proposed to produce microhydrogels (μH) such as radical polymerization in emulsion, selective precipitation of particles, $scCO_2$-based synthesis, and so on (Bordenave, Janaswamy, & Yao, 2014). However, in view of the surface characteristics, μH shows a strong tendency toward aggregation, affecting the properties and consequently the quality of the product. When they are sufficiently dispersed, the particle properties are then reestablished. Ultrasound-assisted emulsion polymerization is an efficient strategy to prepare μH, because it provides an excellent, uniform dispersion of the particles (Campos et al., 2013; Grinberg & Gedanken, 2010; Li, Li, Sun, & Yang, 2013). The ultrasound waves can also contribute to disaggregate particles and prevent coalescence of the emulsion.

This work aims at developing covalent microhydrogel-based composites (μHC) from starch and CNW for application in drug delivery systems via radical polymerization in an ultrasound assisted-emulsion. The drug release profile of μHC was studied by the modeling of the release kinetics of Vitamin B_{12} (Vit-B_{12}), which was used as a model drug. Vit-B_{12} was selected on basis of its hydrophilic characteristics, i.e., it shows affinity for the environment in which it acts (both hydrogel and solvent phases). To obtain covalent μHC, starch and CNW were chemically modified with the purpose of introducing glycidyl methacrylate-derived vinyl groups (GMA) to their polysaccharide backbone. The vinyl bonds on the modified CNW function as potential cross-linking points, allowing the nanowhiskers to be used as a covalent cross-linking agent for vinylated starch. The biocomposites based on the starch/CNW microhydrogels represent an attractive approach for synthesis of new advanced materials that may be used as a design parameter to control the release rate.

2. Experimental

2.1. Materials

Glycidyl methacrylate (GMA, 97%), starch (from corn), poly(vinyl alcohol) (PVA, 87–89% hydrolyzed, Mw = 31,000 g mol^{-1}), vitamin B_{12} and high retention seamless cellulose tubing (average diameter of 15 mm, average flat width of 23 mm, pore sizes of 12,400 MWCO, 99.99% retention) were purchased from Sigma–Aldrich. Benzyl alcohol (99.0%), hexane, toluene, hydrochloric acid and absolute ethyl alcohol (≥99.3%) were supplied by F. Maia.

2.2. Extraction of cellulose from sugarcane bagasse

The sugarcane bagasse was cut into smaller pieces and subsequently washed with water at room temperature while stirring. The samples were left to dry in an oven at 40 °C for 7 days and then crushed with the use of a cutting mill, in the absence of light and humidity. After being washed and dried at room temperature, 100 g of crushed bagasse was submitted to a pretreatment in water, hexane and a toluene/ethanol (2:1) mixture for removal of impurities. Each stage of the treatment was performed at 40 °C for 3 h, and in the interval of each stage, the bagasse was filtered and dried in a ventilated oven at 50 °C for 20 h.

2.3. Synthesis of cellulose nanowhiskers (CNW) from cane-based cellulose

The cellulose nanowhiskers were obtained by acid hydrolysis. For that purpose, 1 g of bagasse-extracted cellulose was added to 25 mL of HCl at 45 °C and left to react for 1 h. Then, the system was cooled to 25 °C and the sample was continually washed until pH 3 was obtained. After hydrolysis, cellulose was dialyzed until neutral pH was reached.

2.4. GMA-based modification of starch (starch$^{\pi}$) and CNW (CNW$^{\pi}$)

Three grams of starch were added to 20 mL of *N*,*N*-dimethylacetamide (DMA) at 100 °C under stirring for 15 min. The thus formed solution was cooled to 50 °C and then 0.05 g of 4-(dimethylamino)pyridine (DMAP), as a catalyst, and 3.0 mL of GMA were introduced. The resulting solution was left to react for 24 h and subsequently precipitated with ethanol. The centrifuged product was washed with ethanol three times to ensure an efficient removal of DMAP and unreacted GMA. The product was left to dry in an oven at 60 °C.

CNW was modified using a strategy comparable to that reported above. Two grams of CNW were added to 20 mL of DMA at 50 °C under stirring for 15 min. Then, 3.0 mL of GMA and 0.05 g of DMAP were added while stirring. After 24 h of reaction, the solution was precipitated with ethanol and subsequently centrifuged. The product was washed with acetone, ethanol and water and left to dry in an oven at 60 °C. The starch$^{\pi}$ and CNW$^{\pi}$ labels were used to identify the modified polysaccharides.

2.5. Preparation of μHC from starch$^{\pi}$ and CNW$^{\pi}$

Five milliliters of a 2.0% (w/v) starch$^{\pi}$ aqueous solution were added to 5.0 mL of a 1.0% (w/v) PVA aqueous solution with 0%, 1%, or 10% CNW$^{\pi}$ at room temperature while stirring. After homogenization, 2.4 mg of ammonium persulfate, as an initiating agent, were introduced and dissolved with help of a magnetic stirrer. Then, benzyl alcohol was added dropwise to the resulting solution so that a two-phase system was formed. The water/benzyl alcohol mixture compositions were used in the 1:4 and 1:3 ratios. The emulsion (w/o) was obtained by sonication with the use of a probe of ultrasonic oscillation (Cole-Parmer® 500, model EW-04711-40), applying a frequency of 20 kHz for 60 s. After that, 150 mL of acetone were added for precipitation. The product was centrifuged and left to dry under vacuum in a desiccator at room temperature for 24 h. In the emulsions without ammonium persulfate (i.e., the control experiment), a longer time was required to induce the radical polymerization, but this led to an overheating.

2.6. Vit-B_{12} release from μHC

Vit-B_{12} (10% in relation to mass of starch$^{\pi}$) was added to μHC-forming emulsion (in situ drug loading approach). This loading strategy was used in view that a significant amount of the drug can be loaded onto the microhydrogel. In such a case, the drug molecules are trapped into the starch network over the cross-linking/polymerization. There is no binding between the modified polysaccharides and Vit-B_{12}. The carbon-carbon double bonds of Vit-B_{12} are connected to either a carbonyl group or chemical groups, which are stabilized by resonances with steric hindrance. Thus, in our present understanding, side reactions of the drug are not possible. For experiments of release, 100 mg of drug-loaded μHC were added to 3.0 mL of a buffer solution at pH 6.9 at 37 °C and subsequently transferred to into a dialysis tube. After being properly sealed, the full tube of the suspension of μHC was fixed

at the bottom of a glass reactor with 220 mL of the same buffer solution equilibrated at 37 °C. The external solution was stirred at 40 rpm using a paddle stirrer, which was positioned 2.5 cm above the dialysis tube. Aliquots of 5.0 mL were collected from the external solution at specified times and transferred to a 1 mm-internal diameter quartz cuvette. The readings of release were done at the wavelength for the maximum absorption of Vit-B_{12} (360 nm) with the use of a UV–vis spectrophotometer (Biochron, Libra S12 model) operating in a spectrophotometric mode. After analysis, the aliquots were returned into the reactor to prevent changes on the volume of the external solution. An analytical curve that correlates the absorption to the concentration of the drug in water ($\varepsilon = 2.3 \times 10^4\ M^{-1}\ cm^{-1}$) was used to determine the concentrations of released Vit-B_{12}.

2.7. Characterizations

2.7.1. Wide-angle X-rays diffraction (WAXD)

The index of apparent crystallinity (IC_{RX}) was determined through the resolutions of the WAXD patterns. The data were recorded on a Siemens Kristaloflex 4-Difractometerusing accelerating voltage of 40 kV, current intensity of 30 mA, 2θ range of 5–50° and scanning speed of $1^\circ\ min^{-1}$, with Ni-filtered Co-K_α radiation at 1.5406 Å. The curves were deconvoluted without a base line by the method of least squares curve-fitting using Lorentzian distribution function, according to Eq. (1):

$$IC_{RX} = 1 - \frac{h_{am}}{h_{cr}} = 1 - \frac{h_{am}}{h_{tot} - h_{am}} \quad (1)$$

where h_{cr} and h_{am} are the maximum intensities (a.u.) of WAXD signal for (0 0 2) crystalline plan at $2\theta = 22.5^\circ$ and for amorphous reflection at $2\theta = 18^\circ$, respectively.

2.7.2. Fourier transform infrared spectroscopy (FTIR)

FTIR spectra of the samples were recorded in a Bomen FT-IR model MB100 spectrometer. Powdered samples were prepared into pellets with KBr. The spectra were acquired in triplicate and a total of 128 scans were run for each spectrum to reach the resolution of $4\ cm^{-1}$.

2.7.3. Scanning electron microscopy

Morphological characteristics of the lyophilized samples were analyzed in a scanning electron microscope (Shimadzu, model SS 550 Superscan). The samples were earlier sputter-coated with a thin layer of gold. SEM images were taken by applying an acceleration voltage of 15 kV and a current intensity of 30 μA.

2.7.4. Transmission electron microscopy (TEM)

TEM images were obtained in a JEM-1400 microscope (JEOL) by applying an acceleration voltage of 120 kV. For TEM imaging, an aliquot of a stirred suspension of microparticles in isopropyl alcohol was added dropwise onto a 400 mesh copper grid.

3. Results and discussion

3.1. Structural characteristics of CNW from cane-based cellulose

Fig. 1 shows the TEM images and WAXD patterns of CNW. The yield of CNW extracted by acid hydrolysis was 62%. CNW showed rod-like morphology. The images suggest structures with an apparent size higher than 500 nm, owing to agglomeration of CNW. This is because CNW prepared from hydrochloric acid hydrolysis were almost charge free (Jiang, Esker, & Roman, 2010; Rusli, Shanmuganathan, Rowan, Weder, & Eichhorn, 2011). The charge free surface leads to a high tendency of the CNW aggregation. The crystalline peaks at 15°, 22.6° and 34.5° (2θ range) provide strong evidences of CNW, corroborating the TEM results. IC_{RX} of CNW, obtained from diffractogram, was 79%.

3.2. Spectroscopic analysis of the modified polysaccharides

Fig. 2 shows the FTIR spectra of starch, starch$^\pi$, CNW, CNW$^\pi$ and μHC. The bands of high intensity at $1716\ cm^{-1}$ in the spectrum of π-CNW (Fig. 2(a)) and at $1722\ cm^{-1}$ in the spectrum of starch$^\pi$ (Fig. 2(a)) were attributed to carbonyl groups (νC=O) of conjugated esters derived from GMA molecules. The bands at $813\ cm^{-1}$ in both the spectra were correlated to =C—H out-of-plane bending. These findings are strong evidences of the addition of chemical groups of GMA to both starch and CNW backbones. The cross-linking/polymerization reaction of starch$^\pi$ with CNW$^\pi$ (gelation) was characterized by the changes of the bands from $1716\ cm^{-1}$ in the spectra of CNW$^\pi$ (Fig. 2(a)) and $1722\ cm^{-1}$ in the spectrum of starch$^\pi$ (Fig. 2(a)) to $1714\ cm^{-1}$ in the spectra of μHC 1% CNW and μHC 10% CNW (Fig. 2(b)). The shifts of those bands are correlated to β-unsaturated conjugation-loss of the ester groups of the GMA moieties, caused by the consumption of the vinyl groups. This argument is strengthened by the disappearance of the vinyl bands at $1650\ cm^{-1}$ (spectrum of CNW$^\pi$) and at $1652\ cm^{-1}$ (spectrum of starch$^\pi$) after the gelation (spectra of μHC), indicating the change from vinylic to methylenic carbons.

3.3. Microparticle morphology

The ultrasound-assisted emulsion cross-linking/polymerization is a powerful approach in the production of small particles. After the modification, starch and CNW were easily dispersed in water, as described in the preparation of μHC. This observation encouraged us to think that, in the emulsion, both modified polysaccharides move toward the aqueous phase and that the particles are therefore formed within the benzyl alcohol-confined water droplets (Reis et al., 2009), which are induced by the acoustic waves. To observe the influence of the composition of the hydroalcoholic emulsion on the microparticle morphology, the 1:3 and 1:4 water/benzyl alcohol mixture ratios were tested. At first, only covalently crosslinked starch particles (that is, without CNW) were prepared in order to evaluate the synthesis medium more appropriate for producing μHC.

Fig. 3 shows the SEM images of covalent starch microparticles produced in the water/benzyl alcohol mixtures in the 1:3 and 1:4 ratios. The (1:3)-based starch particles showed heterogeneous particle dimensions and agglomeration (Fig. 3(a)). Under this condition, the water droplets are close each to other. Therefore, the water–water intermolecular attraction forces increase and the reaction medium coalesces. On the other hand, the (1:4)-based starch particles showed predominantly spherical shape with small size dispersity (Fig. 3(b)). This may be explicated by the larger volume of external phase (benzyl alcohol) that allows the water droplets move as far away as from each to other. Consequently, those water–water attracting forces decrease. The objects of undefined shape in both micrographs were correlated to PVA films.

To further characterize the microparticle dimensions, particle size distribution curves (Fig. 3(a_1) and (b_1)) were elaborated by measuring particle diameters from the respective SEM images (Fig. 3(a) and (b)). The plots correlating number of observations to particle diameter were obtained by a statistical treatment with the use of an Imagen Pro-Plus software version 4.5.0.29. The distribution curve of (1:3)-based starch microparticles showed an average diameter of 0.6 ± 0.2 μm. On the other hand, smaller particles with an average diameter of 0.54 ± 0.2 μm were observed for (1:4) starch microparticles.

On the basis of the SEM results and distribution curves, μHC was produced in the water/benzyl alcohol mixture in the 1:4

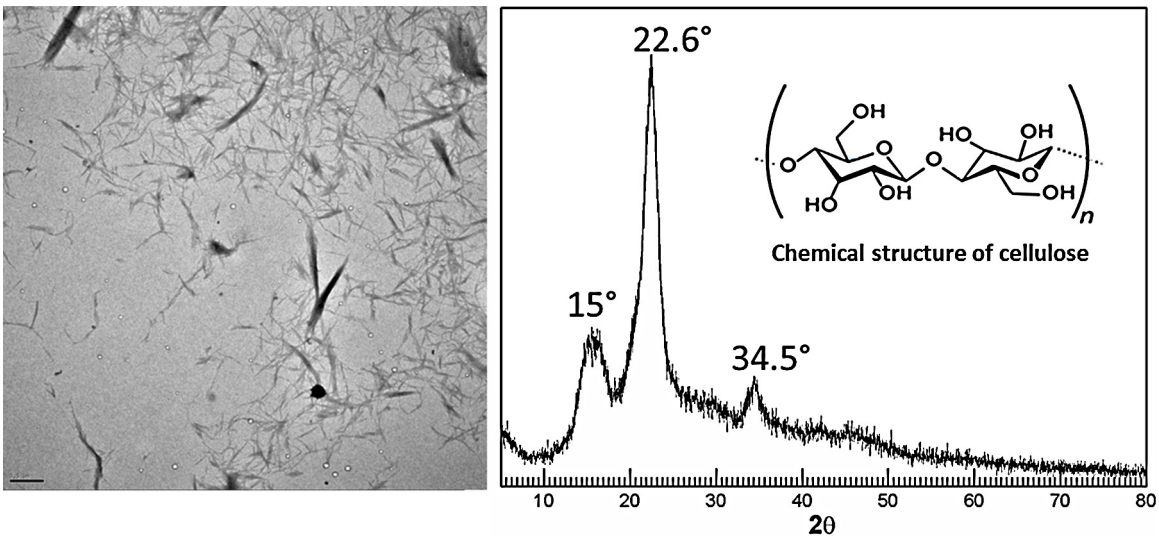

Fig. 1. Bright field TEM images and WAXD patterns of cane-based CNW. Bar charts displaying spatial resolution of 0.5 μm.

proportion. Fig. 4 shows the SEM micrographs of μHC 1% CNW and μHC 10% CNW and the respective particle size distribution curves. μHC 1% CNW (Fig. 4(a)) showed heterogeneous particle dimensions, while μHC 10% CNW (Fig. 3(c)) showed the best results in terms of size dispersity, and sphericity. At high concentrations, CNW may act as an emulsifying agent by adsorption on the water/oil interface, which provides a physical chemical barrier surrounding the droplets and therefore stabilizes the emulsion. CNW is irreversibly adsorbed at the water–oil interface, forming a hydrated layer. Furthermore, Pickering emulsions stabilized by cellulose nanocrystals, which were obtained by hydrochloric acid hydrolysis of bacterial cellulose, have been reported by (Kalashnikova, Bizot, Cathala, & Capron, 2011).

The distribution curves showed the following particle diameter: 0.9 ± 0.3 μm for μHC 1% CNW and 1.4 ± 0.4 μm for μHC 10% CNW. The increase in the average diameter of both μHC compositions, when compared with those of starch-only microparticles, was correlated to contribution of CNW to particle size.

Fig. 5 shows the bright field TEM images of μHC 10% CNW. The TEM images, taken at a spatial resolution of 0.2 μm, showed microparticles with relatively spherical shapes (Fig. 5(a)), which is consistent with SEM results. Although a few morphological features can be identified, TEM images did not showed clear details of the sample. This was correlated to the fact that unstained, transparent materials do not produce contrast when light rays passes through them. As μHC is a low contrast material, most likely due to its polysaccharide structure, the bright field microscope was changed into a dark field microscope in order to create high contrast images. Nevertheless, it was not possible to see small details. Then, the image (bright field) was focused onto a particle and taken at a spatial resolution of 100 nm, as shown in Fig. 5(b). Although the microparticle morphology apparently changed, significant

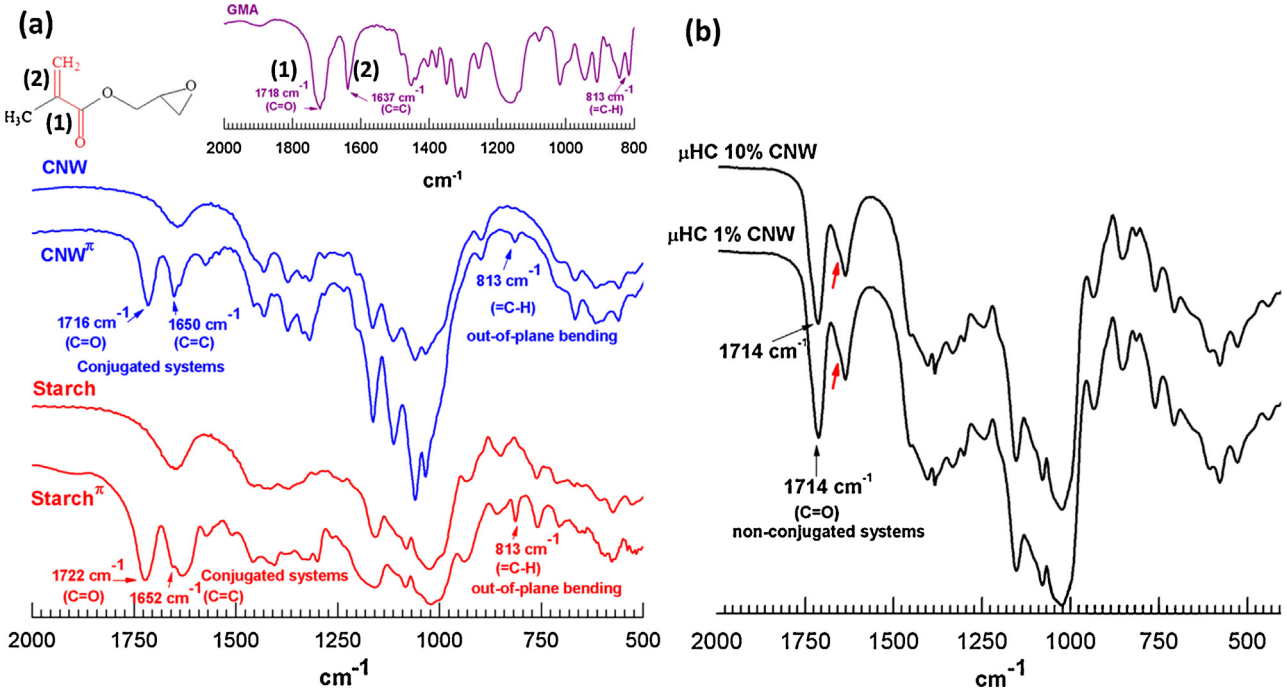

Fig. 2. FTIR spectra of (a) CNW, CNW$^{\pi}$, starch, starch$^{\pi}$, and (b) μHC 1% CNW and μHC 10% CNW in the spectral range of 2000–450 cm^{-1}. *Inset*: FTIR spectrum of GMA.

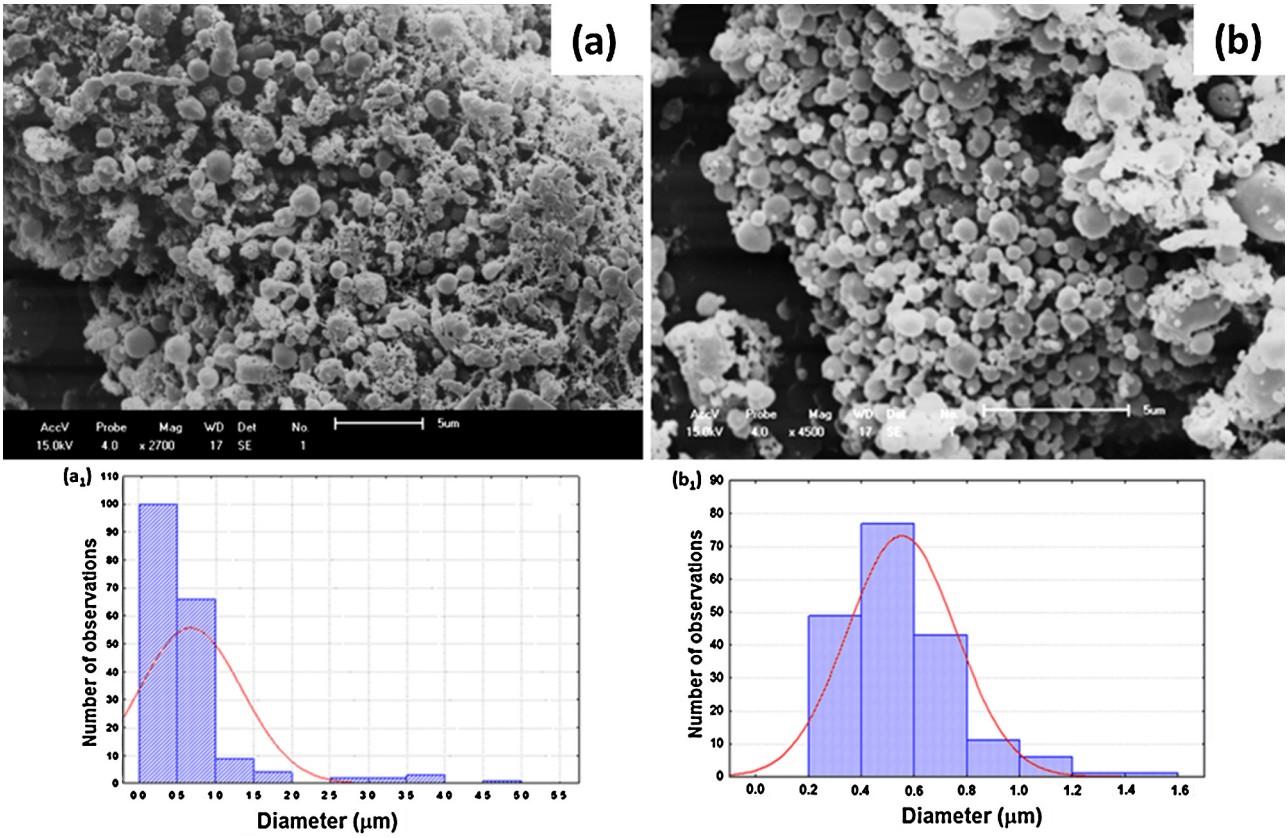

Fig. 3. *Left*: SEM images of covalent starch-onlymicroparticles produced in the water/benzyl alcohol mixtures in the 1:3 (a) and 1:4 (b) ratios. *Right*: respective particle size distribution curves ((a$_1$) and (b$_1$)) obtained by measuring particle diameters of (a) and (b).

information on CNW in the starch particle was given. Starch, which is essentially composed of atoms of carbon, hydrogen and oxygen, corresponds to brightest gray areas. The dark points correspond to rod-like structures of CNW in the microparticle, providing a strong evidence of the formation of the microhydrogel composite.

3.4. Application in drug delivery

The drug release was studied by applying Eq. (2)

$$\frac{C_t}{C_\infty} = kt^n \tag{2}$$

where C_t and C_∞ are the cumulative concentrations of drug released from μHC at a specified time and at equilibrium, respectively, k is a constant of proportionality, and n is the diffusional coefficient that describes the release mechanism.

The Eq. (2) is used to determine the release mechanisms of swellable polymer devices with different geometric forms such as films, cylinders, discs and spheres, but it can predict only the first 60% of released drug.

The values of n depend on geometry of the polymer device, as shown in Table 1. Fickian diffusion indicates that the release mechanism is controlled by diffusion. Anomalous transport is the contribution of both the Fickian diffusional and the relaxational mechanisms. In the case II transport, the mechanism is driven by macromolecular relaxation of the polymer chains, and is independent on time. The super case II transport mechanism results of the contribution of diffusion, macromolecular relaxation, and erosion of the polymer device.

3.5. Release profiles and mechanisms

The drug release performance for starch microparticles, μHC 1% CNW and μHC 10% CNW was studied by plotting curves correlating the fraction of the released drug to time C_t/C_∞, as shown in Fig. 6. The release profile of a microhydrogel is better understood when it is correlated to the time necessary to cumulative release of drug to reach equilibrium (t_∞). This is an important parameter to predict whether the release is sustained for a long time.

The values of t_∞ were summarized in Table 2. μHC showed values of t_∞ longer than that of starch microparticles, and this became more evident for μHC with the larger amount of CNW. It thus becomes clear that the introduction of CNW to starch microparticles leads the drug release to a sustained profile.

Table 1
Values of diffusional exponent, n, for polymer devices with different geometrical shapes.

Diffusional exponent n			Release mechanism
Thin film	Cylinder	Sphere	
0.5	0.45	0.43	Fickian diffusion
$0.5 < n < 1.0$	$0.45 < n < 0.89$	$0.43 < n < 0.85$	Anomalous transport (non-Fickian)
1.0	0.89	0.85	Case II transport (zero-order release)
>1.0	>0.89	>0.85	Super case II transport

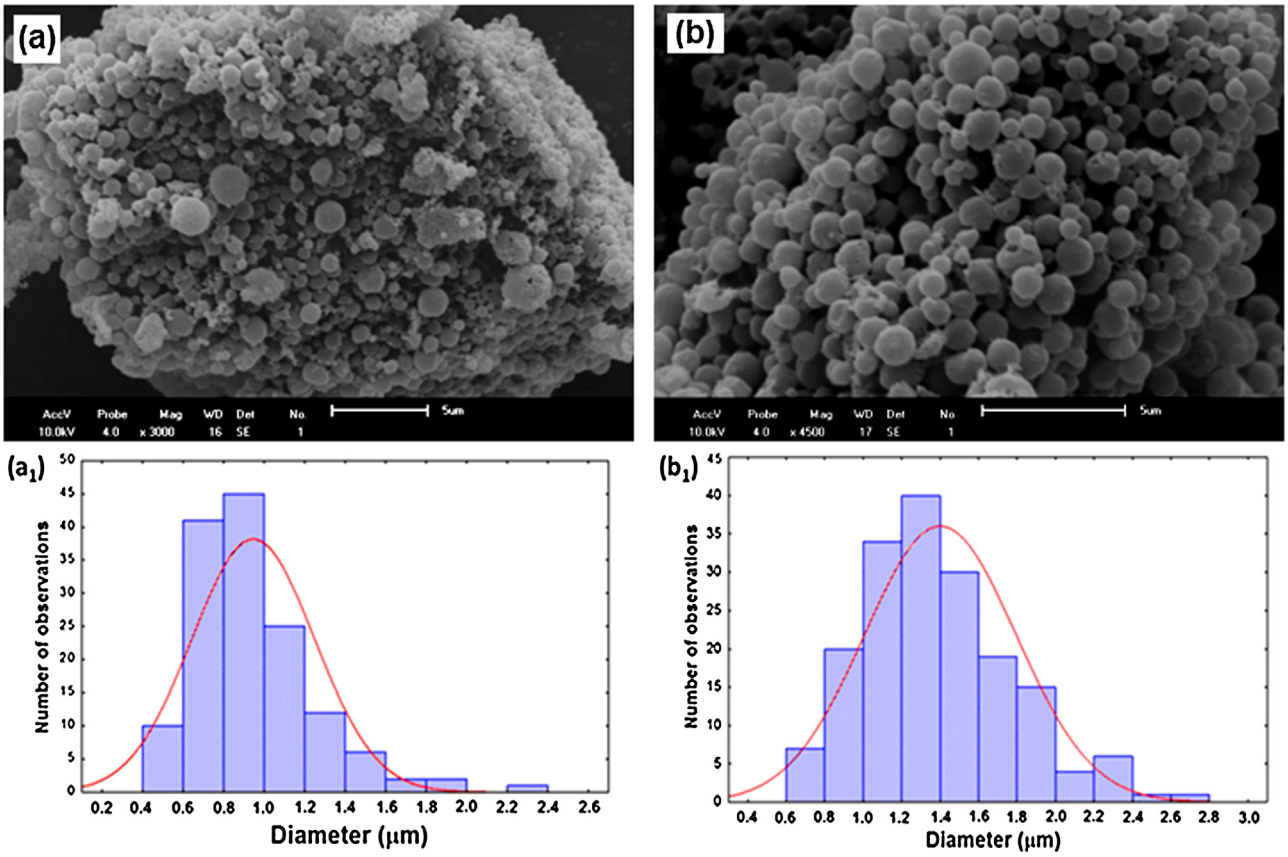

Fig. 4. *Above*: SEM micrographs of μHC 1% CNW and μHC 10% CNW produced in water/benzyl alcohol emulsion in a 1:4 ratio. *Below*: respective particle size distribution curves ((a_1) and (b_1)) obtained by measuring particle diameters of (a) and (b).

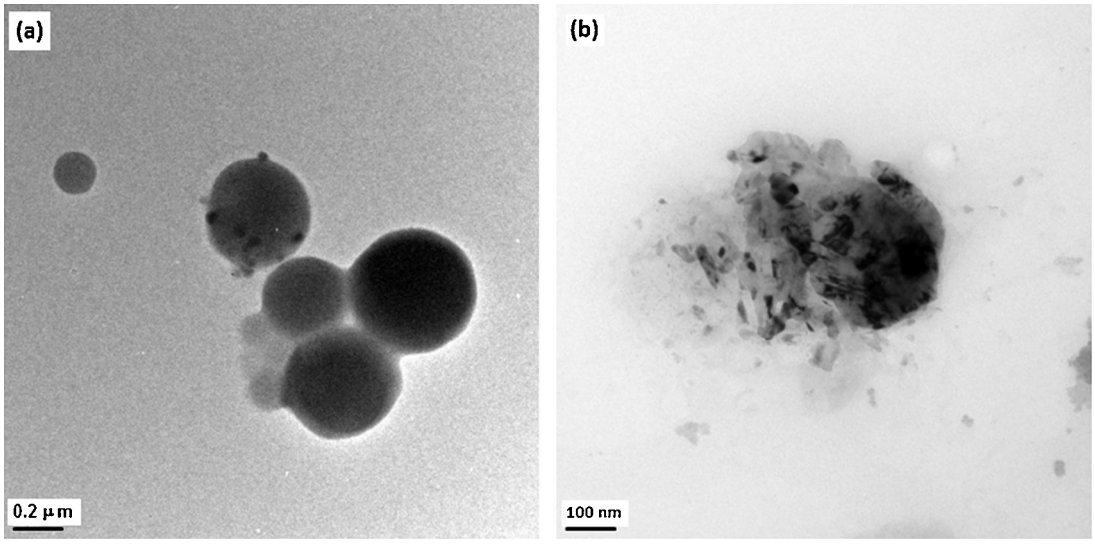

Fig. 5. Bright field TEM image of μHC 10% CNW.

Table 2
Fitting parameters of Eqs. (1) and (2) to Vit-B_{12} release from the from starch-only microparticles, μHC 1% CNW and μHC 10% CNW at 37 °C.

Samples	t_∞ (min)	n	k (10^{-3} min^{-1})	d
Starch microparticles	500 (±12)	0.64 (±0.03) (R^2 = 0.9844)	7.08 (±0.46)	0.89 (±0.07)
μHC 1% CNW	1400 (±63)	0.71 (±0.05) (R^2 = 0.9434)	2.43 (±0.25)	1.63 (±0.33)
μHC 10% CNW	1600 (±39)	0.70 (±0.05) (R^2 = 0.9865)	2.49 (±0.49)	1.23 (±0.14)

The fitting parameters were estimated by a least-squares approach, with a 95% level of confidence using Origin 8.0.

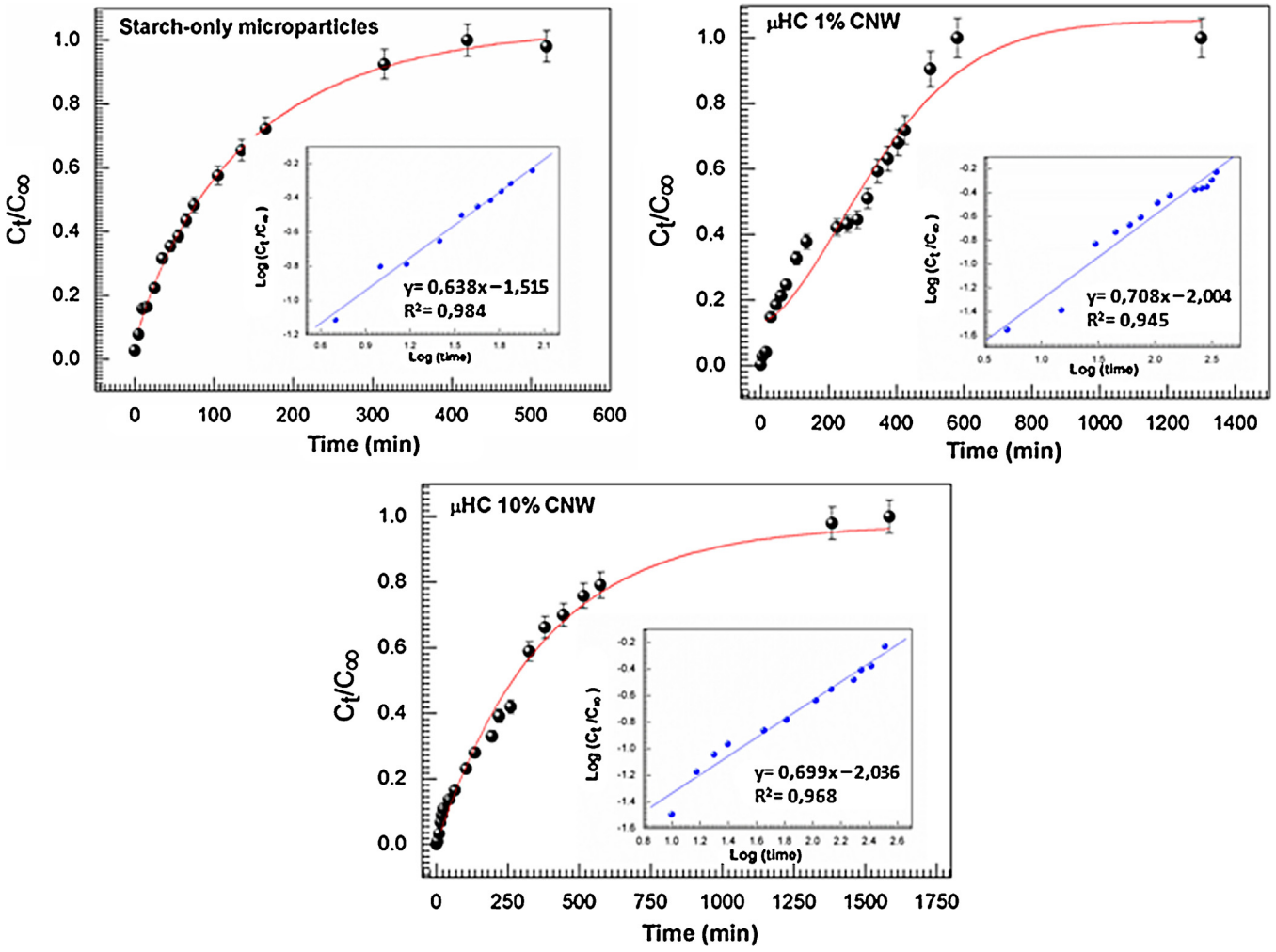

Fig. 6. Time-dependent release curves of Vit-B_{12} from starch-only microparticles, μHC 1% CNW and μHC 10% CNW at 37 °C. The solid lines represent the best fit of release data to Eq. (3). *Inset*: Logarithmical curves of C_t/C_∞ plotted against the time, according to Eq. (2).

The values of n were obtained from slopes of the logarithmical curves of C_t/C_∞ as a function of time for starch microparticles, μHC 1% CNW and μHC 10% CNW (Table 2) and the respective plots were shown in the inset of each Figure. The straight line describes the kinetic model adjusted to first 60% of the released drug. Starch microparticles showed an anomalous mechanism for drug release, contributions of Fickian diffusional and relaxational mechanisms. Both μHC compositions also showed an anomalous mechanism, but with a slight tendency to macromolecular relaxation. It is clear that the release mechanism somewhat responded to changes on the particle architecture. In the other words, adding CNW to starch microparticles leads to differences in the mechanism driving the drug release. From a molecular point of view, it is reasonable to suppose that CNW affected the polymer motion of the network structure of starch.

3.6. Release rate constant (k) of drug

The Eq. (2), in view of its restriction, may not be used to adjust the entire set of the experimental data, being applied only for early times, when the release is linear. In such a case, the results are superficially comprehended and a deep discussion is not possible. To have a further insight into release data it is need to describe the overall profile of the in vitro released drug, which can be assessed by applying a modified version of the Weibull function (Costa & Lobo, 2001):

$$\frac{C_t}{C_\infty} = C_0 + (1 - e^{(-k(t-t_0))^d}) \quad (3)$$

where d and k are constants, respectively. Costa, Valente, Miguel, and Queiroz (2011) reported that d and k are closely related to the mechanism and rate constant of release, respectively (Costa et al., 2011).

The release kinetics of Fig. 6 were adjusted to Eq. (3), from which a value of k and d was described for each fit (Table 2). Notably, both μHC compositions showed release rate approximately 2.9 times slower than the starch microparticles. This means that the addition of CNW to starch microparticles gives a release retardant effect, i.e., when combined with starch, cellulose nanocrystals are a retardant factor for drug release. As a result, the release is extended for longer times, corroborating the data of t_∞. The values of k for μHC 1% CNW and μHC 10% CNW were on the same order of magnitude (also in terms of n), suggesting that the release rate slows until a limit value. From a physical chemical point of view, the decrease in the release rate was attributed to tortuosity effect. This behavior is the result of the disposition of nanocrystals within the polymer device. In other words, the introduction of CNW could produce longer (or tortuous) pathways that would difficult the diffusion of the drug toward the outside microhydrogels.

Values for d higher than 0.8 correspond to n values higher than 0.5 (Kosmidis & Argyrakis, 2003; Kosmidis, Argyrakis, & Macheras, 2003). The analysis of d indicated an anomalous transport for starch microparticles and for both μHC compositions, confirming the mechanism data of Eq. (2).

4. Conclusions

Covalent μHC was produced from CNW and starch for applications in drug delivery. CNW was obtained by acid hydrolysis of cane-based cellulose in hydrochloric acid, demonstrated by WAXD and TEM. The extraction of cellulose from sugarcane bagasse was processed by delignification. Adding vinyl bonds to both CNW and starch allowed us to produce covalent microhydrogels in which the nanocrystals played a role as a covalent cross-linking agent. FTIR indicated that the structure of the hydrogel composite is formed via radical cross-linking/polymerization of CNW$^{\pi}$ with starch$^{\pi}$ because of important spectral changes on the regions of vinyl and carbonyl groups. The morphological properties of the starch microparticles changed following the addition of nanocrystals. μHC with the larger amount of CNW showed the best results in terms of size dispersity, and sphericity. The drug release was regulated in response to changes on the CNW amounts in the starch particle. That became evident when t_{∞} values increased from 500 min (starch microparticles) to 1600 min (μHC 10% CNW), indicating sustained release characteristics. The modeling of the release kinetics indicated that the drug release is driven by anomalous mechanism and that adding CNW to starch microparticles leads to differences in that mechanism. It was also found that the release rate become approximately 2.9 times slower when CNW is added. When combined with starch, the cellulose nanocrystals play a role as a retardant factor for drug release, which is extended for longer times. This is consistent with the data of t_{∞}. The analysis of d confirmed the anomalous mechanism.

Acknowledgments

M.R.M. thanks the Conselho Nacional de Desenvolvimento Científico e Tecnológico (CNPq) for doctorate fellowship. M.R.G. thanks the Coordenação de Aperfeiçoamento de Pessoal de Nível Superior (CAPES/PNPD) for post-doctorate fellowship. A.F.R. acknowledges the financial supports given by CNPq, CAPES, Instituto de Ciência, Tecnologia e Inovação em Materiais Complexos Funcionais (INOMAT) and Fundação Araucária – Brasil.

References

Bordenave, N., Janaswamy, S., & Yao, Y. (2014). Influence of glucan structure on the swelling and leaching properties of starch microparticles. *Carbohydrate Polymers*, *103*, 234–243.

Campos, E., Branquinho, J., Carreira, A. S., Carvalho, A., Coimbra, P., Ferreira, P., et al. (2013). Designing polymeric microparticles for biomedical and industrial applications. *European Polymer Journal*, *49*, 2005–2021.

Chen, X., Huang, L., Sun, H.-J., Cheng, S. Z. D., Zhu, M., & Yang, G. (2014). Stimuli-responsive nanocomposite: Potential injectable embolization agent. *Macromolecular Rapid Communications*, *35*, 579–584.

Costa, D., Valente, A. J. M., Miguel, M. G., & Queiroz, J. (2011). Gel network photodisruption: A new strategy for the codelivery of plasmid DNA and drugs. *Langmuir*, *27*, 13780–13789.

Costa, P., & Lobo, J. M. S. (2001). Modeling and comparison of dissolution profiles. *European Journal of Pharmaceutical Sciences*, *13*, 123–133.

Dufresne, A. (2010). Processing of polymer nanocomposites reinforced with polysaccharide nanocrystals. *Molecules*, *15*, 4111–4128.

Grinberg, O., & Gedanken, A. (2010). The development and characterization of starch microspheres prepared by a sonochemical method for the potential drug delivery of insulin. *Macromolecular Chemistry and Physics*, *211*, 924–931.

Habibi, Y., & Dufresne, A. (2008). Highly filled bionanocomposites from functionalized polysaccharide nanocrystals. *Biomacromolecules*, *9*, 1974–1980.

Ismail, H., Irani, M., & Ahmad, Z. (2013). Starch-based hydrogels: Present status and applications. *International Journal of Polymeric Materials and Polymeric Biomaterials*, *62*, 411–420.

Jiang, F., Esker, A. R., & Roman, M. (2010). Acid-catalyzed and solvolytic desulfation of H_2SO_4-hydrolyzed cellulose nanocrystals. *Langmuir*, *26*, 17919–17925.

Kalashnikova, I., Bizot, H., Cathala, B., & Capron, I. (2011). New pickering emulsions stabilized by bacterial cellulose nanocrystals. *Langmuir*, *27*, 7471–7479.

Klemm, D., Kramer, F., Moritz, S., Lindström, T., Ankerfors, M., Gray, D., et al. (2011). Nanocelluloses: A new family of nature-based materials. *Angewandte Chemie*, *50*, 5438–5466.

Kosmidis, K., & Argyrakis, P. (2003). Fractal kinetics in drug release from finite fractal matrices. *Journal of Chemical Physics*, *119*, 6373–6377.

Kosmidis, K., Argyrakis, P., & Macheras, P. (2003). A reappraisal of drug release laws using Monte Carlo simulations: The prevalence of the Weibull function. *Pharmaceutical Research*, *20*, 988–995.

Li, C., Li, Y., Sun, P., & Yang, C. (2013). Pickering emulsions stabilized by native starch granules. *Colloids and Surfaces A*, *431*, 142–149.

Li, Y., Ko, F. K., & Hamad, W. Y. (2013). Effects of emulsion droplet size on the structure of electrospun ultrafine biocomposite fibers with cellulose nanocrystals. *Biomacromolecules*, *14*, 3801–3807.

Mauricio, M. R., Guilherme, M. R., Kunita, M. H., Muniz, E. C., & Rubira, A. F. (2012). Designing nanostructured microspheres with well-defined outlines by mixing carboxyl-functionalized amylose and magnetite via ultrasound. *Chemical Engineering Journal*, *189–190*, 456–463.

Olivato, J. B., Müller, C. M. O., Carvalho, G. M., Yamashita, F., & Grossmann, M. V. E. (2014). Physical and structural characterization of starch/polyester blends with tartaric acid. *Materials Science and Engineering C*, *39*, 35–39.

Pereira, A. G. B., Fajardo, A. R., Nocchi, S., Nakamura, C. V., Rubira, A. F., & Muniz, E. C. (2013). Starch-based microspheres for sustained-release of curcumin: Preparation and cytotoxic effect on tumor cells. *Carbohydrate Polymers*, *98*, 711–720.

Reis, A. V., Guilherme, M. R., Paulino, A. T., Muniz, E. C., Mattoso, L. H. C., & Tambourgi, E. E. (2009). Synthesis of hollow-structured nano- and microspheres from pectin in a nanodroplet emulsion. *Langmuir*, *25*, 2473–2478.

Rusli, R., Shanmuganathan, K., Rowan, S. J., Weder, C., & Eichhorn, S. J. (2011). Stress transfer in cellulose nanowhisker composites-influence of whisker aspect ratio and surface charge. *Biomacromolecules*, *12*, 1363–1369.

Saboktakin, M. R., Tabatabaie, R. M., Maharramov, A., & Ramazanov, M. A. (2011). Synthesis and in vitro evaluation of carboxymethyl starch–chitosan nanoparticles as drug delivery system to the colon. *International Journal of Biological Macromolecules*, *48*, 381–385.

Shalviri, A., Chan, H. K., Raval, G., Abdekhodaie, M. J., Liu, Q., Heerklotz, H., et al. (2013). Design of pH-responsive nanoparticles of terpolymer of poly(methacrylic acid), polysorbate 80 and starch for delivery of doxorubicin. *Colloids and Surfaces B*, *101*, 405–413.

Sun, Q., Fan, H., & Xiong, L. (2014). Preparation and characterization of starch nanoparticles through ultrasonic-assisted oxidation methods. *Carbohydrate Polymers*, *106*, 359–364.

Valiki, M. R., & Rahneshin, N. (2013). Synthesis and characterization of novel stimuli-responsive hydrogelsbased on starch and L-aspartic acid. *Carbohydrate Polymers*, *98*, 1624–1630.

Wang, Q. Q., Zhu, J. Y., Reiner, R. S., Verrill, S. P., Baxa, U., & McNeil, S. E. (2012). Approaching zero cellulose loss in cellulose nanocrystal (CNC) production: Recovery and characterization of cellulosic solid residues (CSR) and CNC. *Cellulose*, *19*, 2033–2047.

Wu, C., Wang, Z., Zhi, Z., Jiang, T., Zhang, J., & Wang, S. (2011). Development of biodegradable porous starch foam for improving oral delivery of poorly water soluble drugs. *International Journal of Pharmaceutics*, *403*, 162–169.

Zhang, Z., Huang, J., Jiang, S., Liu, Z., Gu, W., Yu, H., et al. (2013). Porous starch based self-assembled nano-delivery system improves the oral absorption of lipophilic drug. *International Journal of Pharmaceutics*, *444*, 162–168.